Tissue Strains Induced in Airways due to Mechanical Ventilation

Ramana M. Pidaparti[*,†] **and Kittisak Koombua**[*‡]

Abstract: Better understanding of the stress/strain environment in airway tissues is very important in order to avoid lung injuries for patients undergoing mechanical ventilation for treatment of respiratory problems. Airway tissue strains responsible for stressing the lung's fiber network and rupturing the lung due to compliant airways are very difficult to measure experimentally. A computational model that incorporates the heterogeneity of the airways was developed to study the effects of airway tissue material properties on strain distributions within each layer of the airway wall. The geometry and boundary conditions of the tissue strain analysis were obtained from the organ-level analysis model. Two sets of airway tissue properties (heterogeneous and homogeneous) were considered in order to estimate the strain levels induced within the tissue. The simulation results showed that the homogeneous model overestimated the maximum strain in the mucosa layer and underestimated the maximum strain in the smooth muscle and cartilage layers. The results of strain levels obtained from the tissue analysis are very important because these strains at the cellular-level can create inflammatory responses, thus damaging the airway tissues.

1   Introduction

Patients with acute lung injury (ALI), acute respiratory distress syndrome (ARDS), airway and other pulmonary diseases often require mechanical ventilation. In the US alone, the incidence of respiratory failures resulting from ventilator-associated lung injury (VALI) is about 137-253 per 100,000 in the general population [1-3]. Mechanical ventilation can be considered as an art more than a science since physicians must balance gas exchange rate and tidal volume to prevent further com-

[*] Department of Mechanical Engineering, Virginia Commonwealth University, Richmond, VA 23284

[†] Reanimation Engineering Shock Center, Virginia Commonwealth University, Richmond, VA 23298

[‡] This paper is a tribute to Prof. Pin Tong in honor of his 72th birthday, and edited by Dr. David Lam.

plications and the ventilator-induced lung injury (VILI) [2]. VILI can be fatal, especially, for ARDS patients in intensive care units (ICU) and might contribute to multiple organ dysfunction syndrome (MODS) from volutrauma, atelectrauma or biotrauma mechanisms [4, 5]. Many techniques have been suggested to prevent VALI by using PEEP and lowering the tidal volume and airway pressure. However, there are some drawbacks. Lowering the tidal volume can cause hypercapnia, decrease aerated lung volume, and increase shunting as well as worsening oxygenation [6]. In addition, PEEP can cause transient oxygen desaturation, hypotension, barotrauma, arrhythmia, and bacterial translocation [7]. Recently, computation models representing airflow in patient specific human lungs have been developed under mechanical ventilation [8]. A greater appreciation now exists of the effects of distending forces on the lung from mechanical ventilation, and how these forces are distributed via the lung's fibrous skeleton [9]. The generation and transmission of the forces due to mechanical ventilation is likely to play a central role in initiating, maintaining, and/or exacerbating new or existing inflammatory responses in the lung.

Airways are of heterogeneous material and composed of many layers, such as mucosa, submucosa, lamina propria, and adventitia [10]. Stiffness in each airway layer also varies [11]. Many *in vitro* and *in vivo* models have been developed to study the effects of mechanical force or pressure on the airways. These models include the cultured airway epithelial cells which were in contact with the cultured fibroblasts via a soluble mediator [12] or fibroblasts suspended in a collagen matrix and bronchial epithelial cells [13]. However, there are some flaws in these models. First, the mechanical force used did not represent the actual force during mechanical ventilation. Second, this model fails to describe the distributions of stresses and strains in each layer of the airway. Since it is very difficult to measure the distributions of stresses and strains in real tissue due to the thinness of each layer in the airways, the computational model that incorporates the heterogeneity of the airways could be very helpful to understand how stresses and strains distribute in each airway layer during mechanical ventilation and avoid lung injury.

In the present study, a computational model that incorporates the heterogeneity of the airways was developed to study the effects of airway tissue material properties on strain distributions within each layer of the airway wall due to mechanical ventilation. Both heterogeneous and homogeneous material models were used to represent airway tissues in order to estimate the strain levels induced within the tissue. The results obtained from the two material models are compared and discussed.

2 Materials and Methods

2.1 Airway Architecture

Airways can be divided into three major layers (mucosa, submucosa, and area outside submocosa) due to their distinct composition and mechanisms through which each layer can be thickened as discussed by Bai et al. [10]. The mucosa consists of epithelium, basement membrane, and lamina propria. The submucosa begins at the outer border of the lamina propria and this region includes the smooth muscle tissue. The area outside the submucosa consists of cartilage-fibrous layer and adventitia. Adventitia is referred to the loose connective tissue that ties the airways to the surrounding environment. Figure 1 shows a schematic diagram of airway wall architecture showing different layers of the airway wall as represented by Kamm [11].
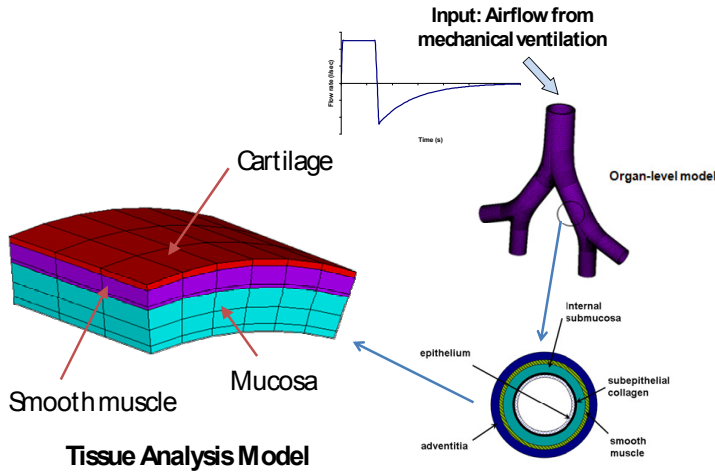

Figure 1: An overview of the tissue – analysis model with input of airflow due to mechanical ventilation from organ level model

2.2 Governing Equations and Computational Method

The governing equations for strain distributionsin each layer of the airway wall during mechanical ventilation are the steady state structural equations and are described below using Einstein's repeated index convention [14].

Equation of motion

$$\frac{\partial \sigma_{ij}}{\partial x_j} + F_i = 0 \tag{1}$$

Constitutive relations

$$\sigma_{ij} = C_{ijkl}\varepsilon_{kl} \tag{2}$$

In the equations above, σ is the stress in each direction, F is the body force, ρ is density, C is the elasticity tensor, and ε is the strain in each direction. The finite element method was chosen to solve these governing equations employing the commercial finite element software, ANSYS [15].

Table 1: Material properties of each layer in the airway wall tissue

Airway wall layer	Young's modulus (kPa)	
Mucosa (Yamada, [20])	Circumferential	80
	Longitudinal	150
Smooth muscle with cartilage (Jiang and Stephens, [21])	Circumferential	75
	Longitudinal	75

2.3   Computational Models and Boundary Conditions

The tissue geometry was obtained from the center of the airway generation 4. Figure 1 shows airway architecture along the thickness of the bronchial wall and the corresponding computation domain for tissue analysis. For tissue analysis model, the airway wall was treated as a composite material. Each layer of the airway tissue is assumed to be linear elastic and perfectly bonded to other layers. The material properties for each layer are tabulated in Table 1, and a major Poisson's ratio of 0.45 was used for all the layers. Thickness of each layer is obtained from the histological section of airway tissue [16] and it is 240, 115, and 55 mm for mucosa, smooth muscle, and cartilage layer, respectively.

Figure 2 shows the computational domain used for the tissue analysis. The computational domain of the airway tissue is modeled in the finite element software, ANSYS [15] with solid elements, BRICK45 representing each layer of the airway tissue. At least three elements are used in the thickness direction of each layer to make sure that strain variations in thickness direction can be captured. In the simulations, small deformations are assumed, however, for realistic model, large
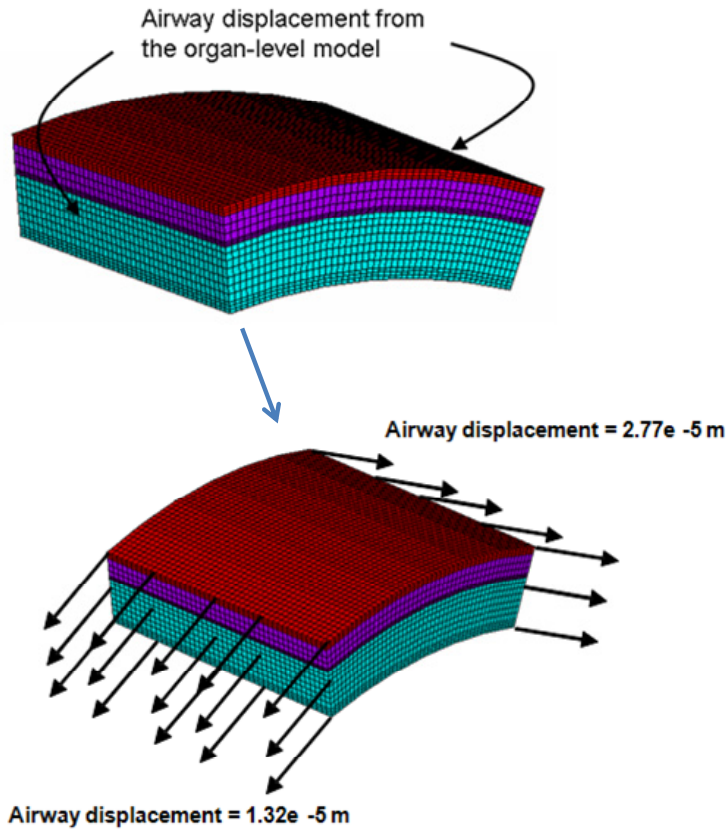
Figure 2: The finite element model and boundary conditions that were used for tissue analysis. The airway displacements used in the analysis were from airway displacement at the organ-level at the end of inhalation with 60-L/min constant flow waveform.

deformations need to be considered. The boundary conditions for the tissue analysis are airway displacements at each location from the organ-level model due to mechanical ventilation and shown in Fig. 2. The displacements at the end of inhalation for 60-l/min constant flow waveform were chosen for the tissue stress analysis based on a previous fluid-solid analysis of compliant airways due to mechanical ventilation [17].

The effect of material properties on the strain distributions in each layer was investigated using two material models: heterogeneous and homogeneous material models. The analysis was performed to study distributions of von Mises strain,
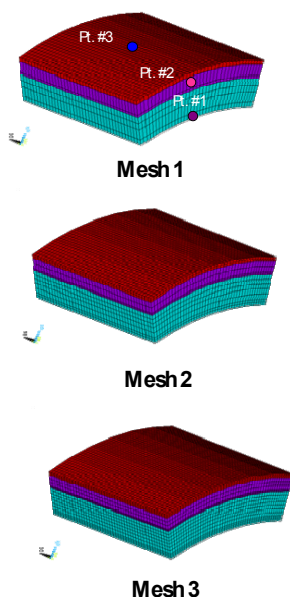
Figure 3: Finite element meshes considered for convergence study in tissue analysis

normal strain, and shear strain in each airway layer. The von Mises strain is an average strain at any point. It is a combination of normal and shear strain in all directions [18].
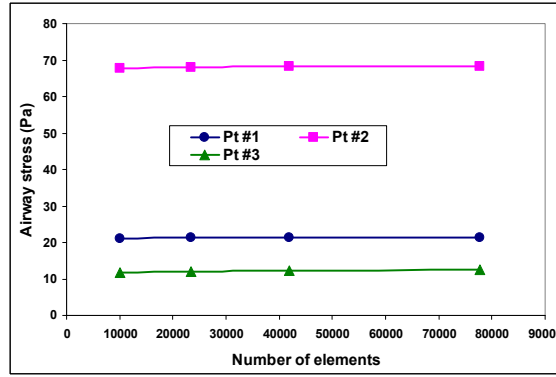
3 Results

3.1 *Convergence Study*

A review of the literature indicates that there is no information of strain distributions in each airway layer during mechanical ventilation. Therefore, a mesh-independence study was performed to confirm that a fine enough element had been used to represent the computational domain. Changes in displacement and von Mises stress were used as convergence criteria. A converged model is obtained when changes in these criteria are less than 5%. Typical meshes used for convergence is shown in Fig. 3. The results of convergence on displacement as well as von-Mises stress with increasing number of elements in the analysis model are shown in Figure 4. It can be seen from Fig. 4 that the converged mesh (Mesh 3 in Fig. 3) was used for obtaining the results from tissue analysis.
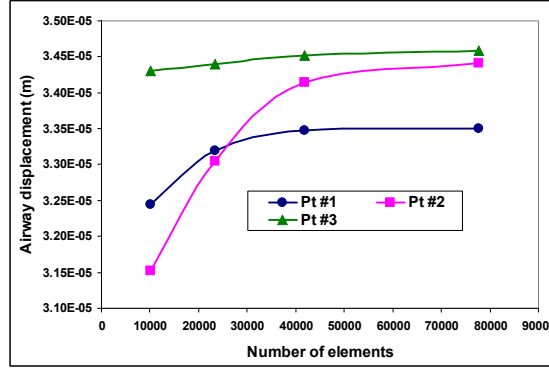
(a)

(b)

Figure 4: Results of airway displacement and stress with increasing number of finite elements in the tissue analysis model

3.2 Homogeneous Tissue Properties Prediction

Material properties of the homogeneous airway wall for tissue analysis as well as for organ-level modeling can be calculated using material properties of each tissue layer and a simple composite-material theory [19].

$$E = v_{mu\cos a}E_{mu\cos a} + v_{SM}E_{SM} + v_{cartilage}E_{cartilage} \qquad (3)$$

In the above equation, E is a Young's modulus of elasticity of the homogeneous airway wall, $E_{mu\cos a}$ is a Young's modulus of elasticity of the mucosa, E_{SM} is a Young's modulus of elasticity of the smooth muscle, $E_{cartilage}$ is a Young's modulus

Heterogeneous model

-.001099
.834E-03
.002768
.004701
.006634
.008568
.010501
.012434
.014368
.016301

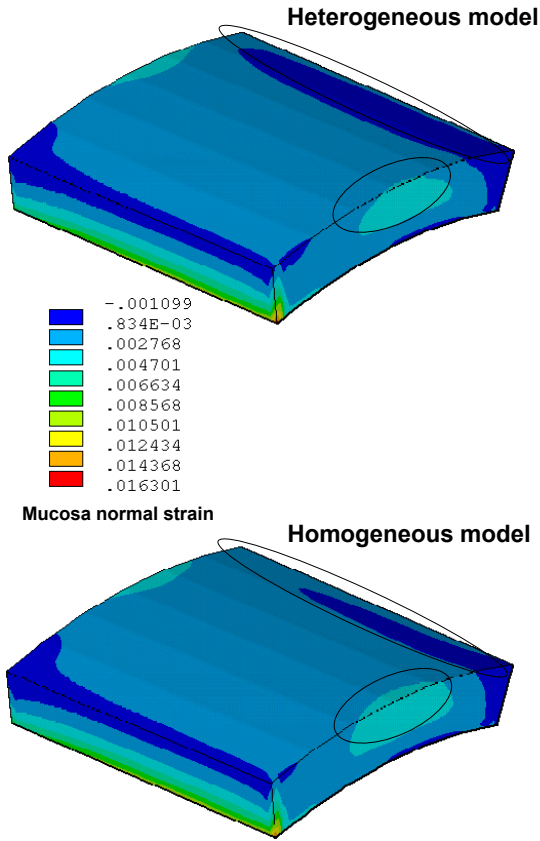**Mucosa normal strain**

Homogeneous model

Figure 5: Normal strain distributions in the mucosa layer for the heterogeneous model (top) and homogeneous model (bottom). Circles indicate the difference in the strain distributions

of elasticity of the cartilage, v_{mucosa} is a volume fraction of the mucosa, v_{SM} is a volume fraction of the smooth muscle, and $v_{cartilage}$ is a volume fraction of the cartilage. The volume fraction of each layer is a ratio of the thickness in each layer to total thickness of the airway tissue.

Substituting values of the Young's modulus of elasticity and the volume fraction for each layer into (3), we obtain

In a circumferential direction

$$E = \frac{240}{410}(80) + \frac{115}{410}(75) + \frac{55}{410}(75) = 78 \quad kPa$$

Heterogeneous model


```
-.003888
-.00286
-.001832
-.804E-03
.224E-03
.001251
.002279
.003307
.004335
.005363
```

Smooth muscle normal strain
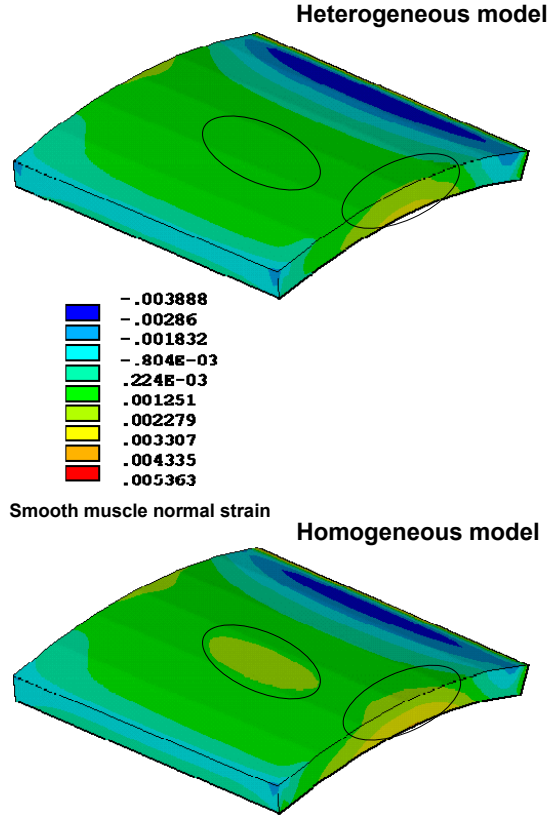
Homogeneous model

Figure 6: Normal strain distributions in the smooth muscle layer for the heterogeneous model (top) and homogeneous model (bottom). Circle indicates the difference in the strain distributions.

In a longitudinal direction

$$E = \frac{240}{410}(150) + \frac{115}{410}(75) + \frac{55}{410}(75) = 120 \quad kPa$$

As can be seen, material properties calculated from the composite-material theory are in good agreement with material properties calculated from the stress-strain curve of the whole airways [22, 23].

3.3 Normal Strain Distributions

The normal strain distributions in the mucosa layer for both models are shown in Figure 5. As can be seen from this figure, the distributions of normal strain in the

mucosa layer for both material models are different. High normal strain areas from the heterogeneous model are smaller than those from the homogeneous model. The maximum normal strain in the mucosa layer from the heterogeneous model was higher than that for the homogeneous model. This maximum was 1.6% and 1.5% for the heterogeneous model and homogeneous model, respectively. The maximum normal strain in the smooth muscle layer from the heterogeneous model was lower than that for the homogeneous model. This maximum was 0.48% and 0.53% for the heterogeneous model and homogeneous models, respectively. The distributions of normal strain in the smooth muscle layer for both models were also different. High normal strain areas from the heterogeneous model were smaller than those from the homogeneous model (see Figure 6). The normal strain distributions in the cartilage layer for both models are shown in Figure 7. The maximum normal strain in the cartilage layer from the heterogeneous model was higher than that for the homogeneous model since the cartilage layer in the heterogeneous model is less stiff than that in the homogeneous model. This maximum was 1.10% and 0.99% for the heterogeneous model and homogeneous model, respectively. The distributions of normal strain in the cartilage layer from both models were also different. High normal strain areas from the heterogeneous model were smaller than those from the homogeneous model.

3.4 Shear Strain Distributions

The shear strain distributions in the mucosa layer for both models are shown in Figure 8. As can be seen from this figure, the distributions of shear strain in the mucosa layer for both material models are different. High shear strain areas from the heterogeneous model were smaller than those from the homogeneous model. The maximum shear strain in the mucosa layer from the heterogeneous model was lower than that for the homogeneous model since the mucosa layer in the heterogeneous model is stiffer than that in the homogeneous model. This maximum was 2.1% and 2.3% for the heterogeneous model and homogeneous models, respectively. The maximum shear strain in the smooth muscle layer from the heterogeneous model was greater than that for the homogeneous model since the smooth muscle layer in the heterogeneous model is less stiff than that in the homogeneous model. This maximum was 1.9% and 1.8% for the heterogeneous model and homogeneous model, respectively. The distributions of shear strain in the smooth muscle layer for both models were also different. High shear strain areas from the heterogeneous model were bigger than those from the homogeneous model (see Figure 9). The shear strain distributions in the cartilage layer for both models are shown in Figure 10. The maximum shear strain in the cartilage layer from the heterogeneous model was greater than that for the homogeneous model since the cartilage

Heterogeneous model


```
-.010603
-.008349
-.006095
-.003841
-.001587
.667E-03
.002921
.005175
.007429
.009683
```

Cartilage normal strain
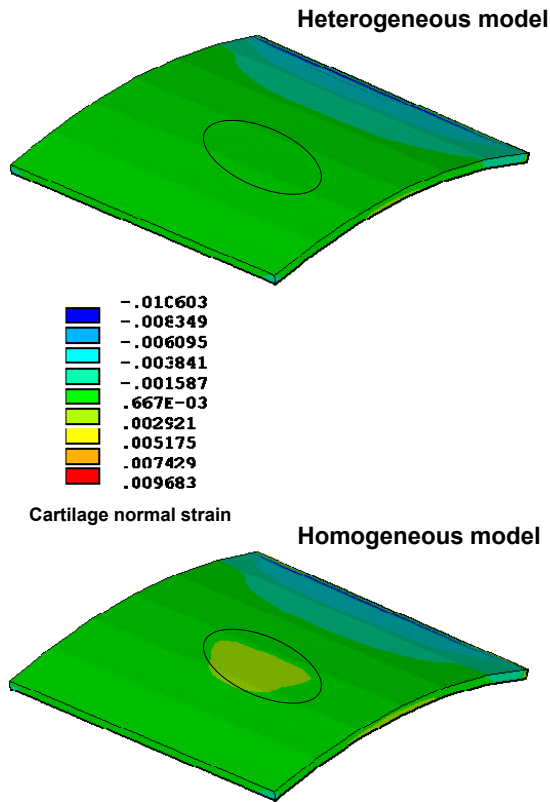
Homogeneous model

Figure 7: Normal strain distributions in the cartilage layer for the heterogeneous model (top) and homogeneous model (bottom). Circle indicates the difference in the strain distributions

layer in the heterogeneous model is less stiff than that in the homogeneous model. This maximum was 2.8% and 2.6% for the heterogeneous model and homogeneous models, respectively. The distributions of shear strain in the cartilage layer from both models were also different. High shear strain areas from the heterogeneous model were bigger than those from the homogeneous model.

3.5   *Von-Mises Strain Distributions*

The von Mises strain distributions in the mucosa layer for both models (heterogeneous and homogeneous) are shown in Figure 11. As can be seen from this figure, the distributions of von Mises strain in the mucosa layer for both material
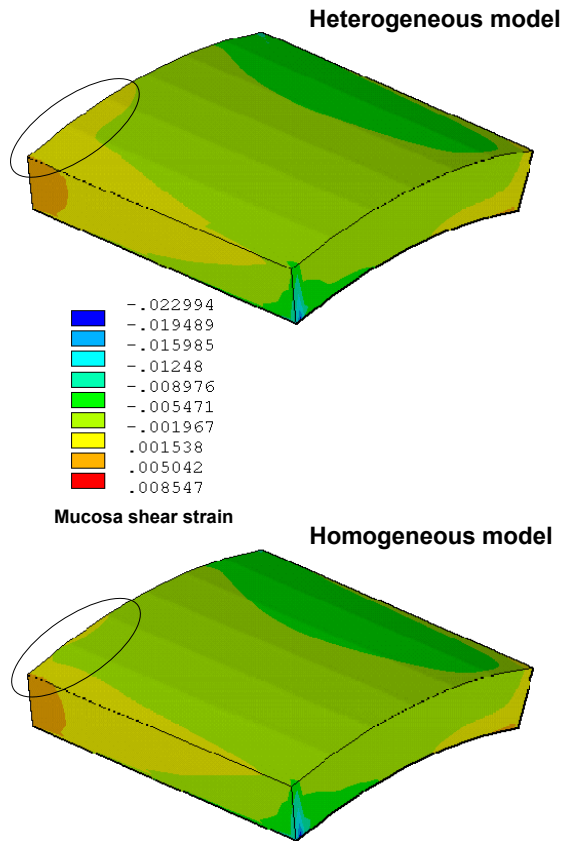
Figure 8: Shear strain distributions in the mucosa layer for the heterogeneous model (top) and homogeneous model (bottom). Circle indicates the difference in the strain distributions

models are different. High von Mises strain areas from the heterogeneous model were smaller than those from the homogeneous model. The maximum von Mises strain in the mucosa layer from the heterogeneous model was lower than that for the homogeneous model since the mucosa layer in the heterogeneous model is stiffer than that in the homogeneous model. This maximum was 1.8% and 2.0% for the heterogeneous model and homogeneous models, respectively.

The maximum von Mises strain in the smooth muscle layer from the heterogeneous model was greater than that for the homogeneous model since the smooth muscle

Heterogeneous model

■ (blue)	-.019028
■	-.016602
■	-.014175
■	-.011749
■	-.009323
■	-.006896
■	-.00447
■	-.002044
■	.383E-03
■ (red)	.002809

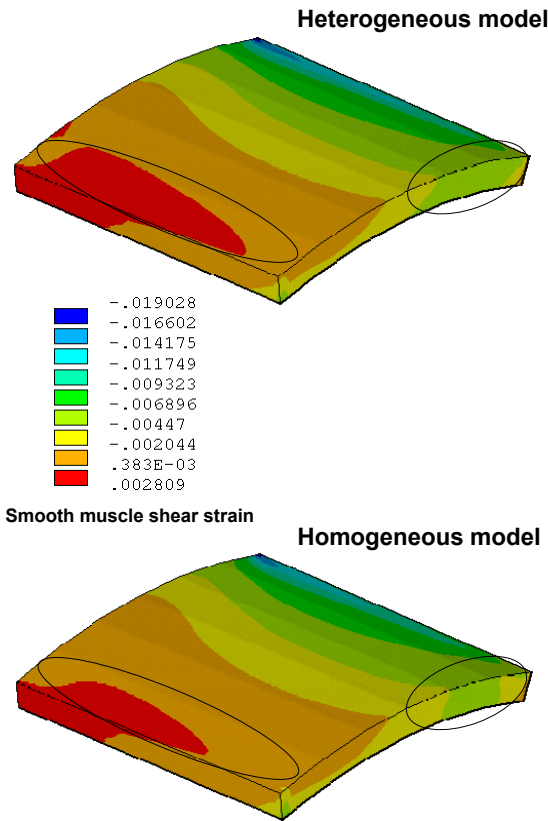**Smooth muscle shear strain**

Homogeneous model

Figure 9: Shear strain distributions in the smooth muscle layer for the heterogeneous model (top) and homogeneous model (bottom). Circle indicates the difference in the strain distributions

layer in the heterogeneous model is less stiff than that in the homogeneous model. This maximum was 2.5% and 2.2% for the heterogeneous model and homogeneous model, respectively. The distributions of von Mises strain in the smooth muscle layer for both models were also different. High von Mises strain areas from the heterogeneous model were bigger than those from the homogeneous model (see Figure 12). The von Mises strain distributions in the cartilage layer for both models are shown in Figure 13. The maximum von Mises strain in the cartilage layer from the heterogeneous model was greater than that for the homogeneous model since the cartilage layer in the heterogeneous model is less stiff than that in the

Heterogeneous model

```
-.027968
-.024559
-.021151
-.017742
-.014333
-.010925
-.007516
-.004107
-.699E-03
.00271
```

Cartilage shear strain
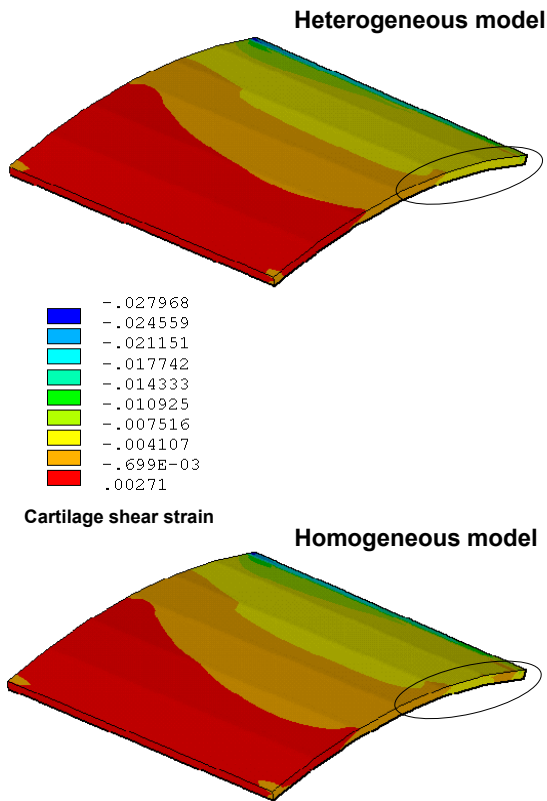
Homogeneous model

Figure 10: Shear strain distributions in the cartilage layer for the heterogeneous model (top) and homogeneous model (bottom). Circle indicates the difference in the strain distributions

homogeneous model. This maximum was 3.7% and 3.1% for the heterogeneous model and homogeneous model, respectively. The distributions of von Mises strain in the cartilage layer from both models were also different. High von Mises strain areas from the heterogeneous model were bigger than those from the homogeneous model.

4 Discussion

A computational model that incorporates the heterogeneity of the airways was developed to study strain distributions in each airway layer of the airway tissue. This

Heterogeneous model

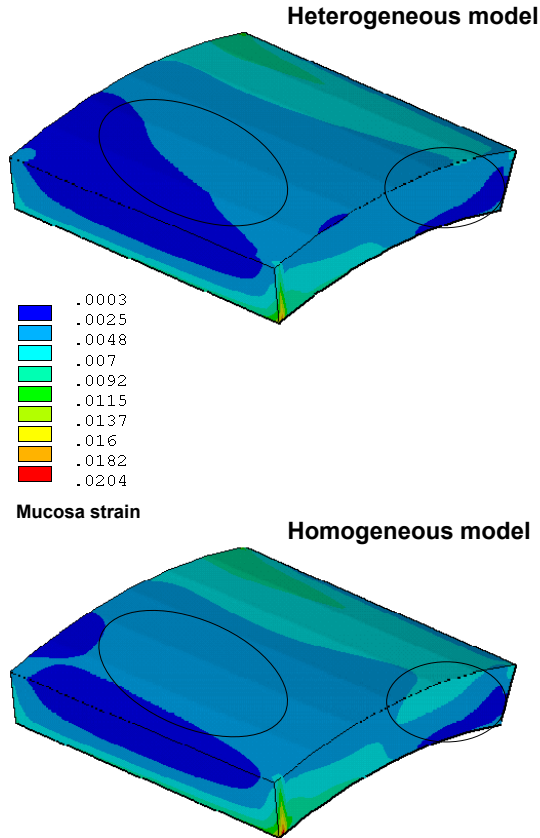|	
■	.0003
■	.0025
■	.0048
■	.007
■	.0092
■	.0115
■	.0137
■	.016
■	.0182
■	.0204

Mucosa strain

Homogeneous model

Figure 11: von Mises strain distributions in the mucosa layer for the heterogeneous model (top) and homogeneous model (bottom). Circles indicate the difference in the strain distributions

is due to the fact that each layer in the airways is extremely thin and also, it is very difficult to measure the strain distributions in the real tissue. The effect of the material model on strain distributions in each airway layer was investigated using heterogeneous and homogeneous material models. The simulation results showed that the material model greatly affected the strain distributions in the airway as well as the maximum strain in each airway layer. Overall, the homogeneous material model overestimated the maximum strain level in the mucosa layer by about 11% and underestimated the maximum strain level by about 12% and 16% in the smooth muscle and cartilage layer, respectively. It is very interesting to note that there were both normal and shear strain components in each layer although the
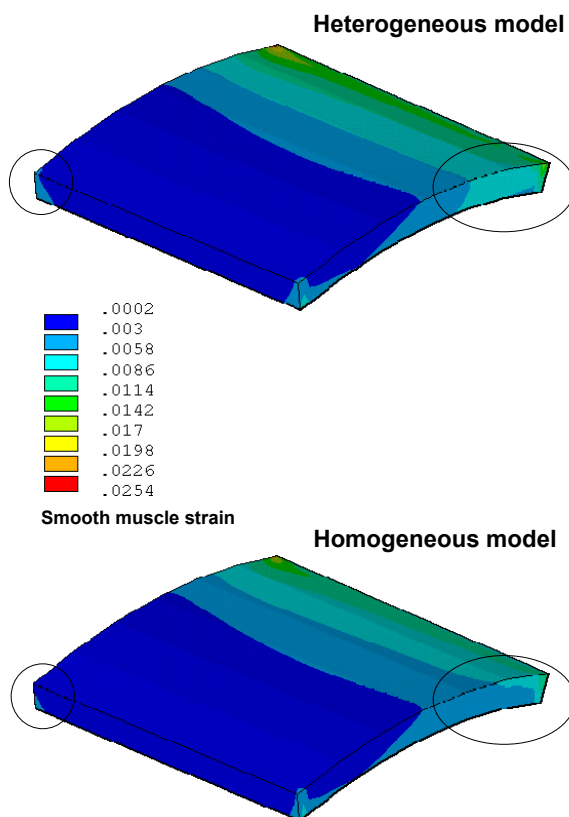
Heterogeneous model

Figure 12: von Mises strain distributions in the smooth muscle layer for the heterogeneous model (top) and homogeneous model (bottom). Circle indicates the difference in the strain distributions

airway displacement from the organ-level model was in the normal direction.

The importance of strains in the airways is that these strain levels can activate neutrophils via release of interleukin (IL)-8 without cell injury. An experiment with alveolar epithelial cells showed that cells with 10-15% linear strain released IL-8 about 8-49% more than the normal cells [24]. Strain level also acted synergistically with activated eosinophils to induce upregulation of gene in airway remodeling in diseases such as asthma [25, 26]. In addition, strain caused cell injury [27, 28], apotosis [29] and necrosis [29]. Therefore, it is very important to incorporate the heterogeneity of the airway into the computational model at the tissue level so that the strain level in each airway layer can be accurately obtained.

Heterogeneous model


```
     .0001
     .0042
     .0083
     .0124
     .0165
     .0206
     .0247
     .0288
     .0328
     .0369
```
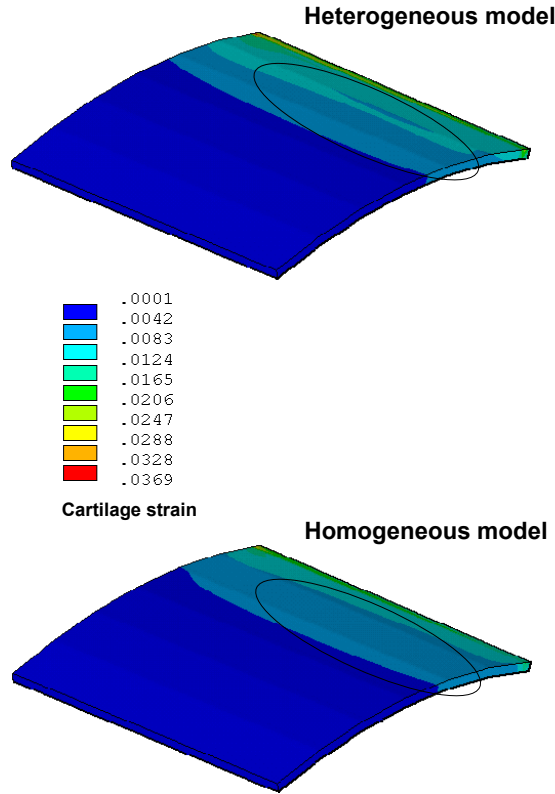
Cartilage strain

Homogeneous model

Figure 13: von Mises strain distributions in the cartilage layer for the heterogeneous model (top) and homogeneous model (bottom). Circle indicates the difference in the strain distributions

5   Conclusions

A tissue-level model was developed to study the strain distributions in each layer of the airway tissue. The geometry and boundary conditions of the tissue analysis model were obtained from the organ-level model. The finite element method was chosen to solve the continuum model used to describe the distributions of strain in the airway tissue. The effect of material properties on the strain distributions was investigated, assuming that the airway tissue is either heterogeneous or homogeneous. The simulation results showed that the homogeneous model overestimated the maximum strain in the mucosa layer; however the homogeneous model underestimated the maximum strain in the smooth muscle and cartilage layers. Since the strain levels obtained from the tissue analysis model can be transferred to the

cellular-level that induces inflammatory responses, it is important to treat the airway tissue as a heterogeneous material, where distributions of strains in each layer are considered.

References

1. Sather JE, Schuur JD. Epidemiology of acute respiratory failure and mechanical ventilation in U.S. emergency departments, 1993-2004. Annals of Emergency Medicine 2007; 50:S110.

2. Rubenfield, G.D., Caldwell, E., Peabody, E., Weaver, J., Martin, D. P., Neff, M., Stern, E.J., and Hudson, L.D., 2005, "Incidence and Outcomes of Acute Lung Injury," N. Engl. J. Med., 353, pp. 1685-1693.

3. Behrendt CE. Acute respiratory failure in the United States: Incidence and 31-day survival. Chest 2000;118:1100-5.

4. Imai Y, Slutsky AS. Systemic Effects of Mechanical Ventilation. In: Dreyfuss D, Saumon G, Hubmayr RD, eds. Ventilator-Induced Lung Injury. New York, NY: Taylor & Francis Group; 2006:267-85.

5. Khadaroo RG, Marshall JC. ARDS and the multiple organ dysfunction syndrome: Common mechanisms of a common systemic process. Critical Care Clinics 2002;18:127-41.

6. Tobin MJ. Advances in Mechanical Ventilation. The New England Journal of Medicine 2001;344:1986-96.

7. Fan E, Needham DM, Stewart TE. Ventilatory Management of Acute Lung Injury and Acute Respiratory Distress Syndrome. JAMA 2005;294:2889-96.

8. Comeford, A., Forster, C., and Wall, W. A., "Structured Tree Imnpedance Outflow Boundary Conditions for 3D Lung Simulations, ASME J. of Biomechanical Engineering, 2010, 132, pp. 081002-1-10.

9. Gattinoni L, Carlesso E, Cadringher P, Valenza F, Vagginelli F, Chiumello D. Physical and Biological Triggers of Ventilator-induced Lung Injury and its Prevention. European Respiratory Journal 2003;47 (suppl.):15S-25S.

10. Bai A, Eidelman D H, Hogg J C, James A L, Lambert R K, Ludwig M S, Martin J, Mcdonald D M, Mitzner W A, Okazawa M, Pack R J, Pare P D, Schellenberg R R, Tiddens H A W M, Wagner E M, and Yager D, 1994. Proposed Nomenclature for Quantifying Subdivisions of the Bronchial Wall. Journal of Applied Physiology 77, 1011-1014.

11. Kamm R D, 1999. Airway wall mechanics. Annual Review of Biomedical Engineering 1, 47-72.

12. Swartz M A, Tschumperlin D J, Kamm R D, and Drazen J M,

13. Mechanical Stress is Communicated between Different Cell Types to Elicit Matrix Remodeling. PNAS 98, 6180-6185.

14. Choe M M, Sporn P H S, and Swartz M A, 2003. An in vitro airway wall model of remodeling. American Journal of Physiology: Lung Cellular and Molecular Physiology 285, L427-L433.

15. Reddy J N 1993 An Introduction to the Finite Element Method 2 edn McGraw-Hill, New York, NY.

16. ANSYS 2005 ANSYS 10.0 User Guide ANSYS Inc., Canonsburg, PA

17. Benayoun L, Druilhe A, Dombret M, Aubier M, and Pretolani M, 2003. Airway Structural Alterations Selectively Associated with Severe Asthma. American Journal of Respiratory and Critical Care Medicine 167, 1360-1368.

18. Koombua, K., Pidaparti, R. M., Longest, P. W., and Ward,K. R. 2009 Biomechanical Aspects of Compliant Airways due to Mechanical Ventilation, Molecular and Cellular Biomechanics, Vol. 6, #4, Vol. pp.203-216.

19. Dowling N E 1998 Mechanical Behavior of Materials 2 edn Prentice Hall, Upper Saddle River, NJ.

20. Barbero E J 1999 Introduction to Composite Materials Design Taylor & Francis, Inc., Philadelphia, PA.

21. Yamada H, 1970. Mechanical Properties of Respiratory and Digestive Organs and Tissues. In: Evans F G (ed.), Strength of Biological Materials. Williams & Wilkins, Baltimore, MD, p. 145.

22. Jiang H and Stephens N L, 1990. Contractile properties of bronchial smooth muscle with and without cartilage. Journal of Applied Physiology 69, 120-126.

23. Croteau, J. R. and Cook, C. D., 1961. Volume-pressure and Length-tension Measurements in Human Tracheal and Bronchial Segments. Journal of Applied Physiology 16, 170-172.

24. Prakash, U. B. S. and Hyatt, R. E., 1978. Static Mechanical Properties of Bronchi in Normal Excised Human Lungs. Journal of Applied Physiology 45, 45-50.

25. Vlahakis N E, Schroeder M A, Limper A H, and Hubmayr R D, 1999. Stretch Induces Cytokine Release by Alveolar Epithelial Cells In Vitro. American Journal of Physiology: Lung Cellular and Molecular Physiology 277, L167-L173.

26. Choe M M, Sporn P H S, and Swartz M A, 2003. An in vitro airway wall model of remodeling. American Journal of Physiology: Lung Cellular and Molecular Physiology 285, L427-L433.

27. Haseneen N A, Vaday G G, Zucker S, and Foda H D, 2002. Mechanical Stretch Induces MMP-2 Release and Activation in Lung Endothelium: Role of EMMPRIN. American Journal of Physiology: Lung Cellular and Molecular Physiology 284, L541-L547.

28. Tschumperlin D J and Margulies S S, 1998. Equibiaxial deformation-induced injury of alveolar epithelial cells in vitro. American Journal of Physiology: Lung Cellular and Molecular Physiology 275, L1173-L1183.

29. Tschumperlin D J, Oswari J, and Margulies S S, Deformation-induced injury of alveolar epithelial cells. Effect of frequency, duration, and amplitude. American Journal of Respiratory and Critical Care Medicine 162, 357-362.

30. Hammerschmidt S, Kuhn H, Grasenack T, Gessner C, and Wirtz H, 2004. Apoptosis and Necrosis Induced by Cyclic Mechanical Stretching in Alveolar Type II Cells. American Journal of Respiratory Cell And Molecular Biology 30, 396-402.